Wideband Transformers: An Intuitive Approach to Models, Characterization and Design

By Chris Trask
Sonoran Radio Research

Wideband transformers constructed with high permeability ferrite and powdered iron magnetic materials are used extensively for impedance matching, power combining and power splitting, as well as other functions, for frequencies ranging from VLF to VHF. Despite this broad range of uses, a concise step-by-step procedure for characterizing wideband transformers and effecting a design making full use of the parasitic reactances is lacking.

This article presents such a procedure as well as discusses the development of the equivalent circuit of the wideband transformer. The new procedure aims to provide the designer with a means for obtaining an intuitive understanding of the limitations and compromises.

Ideal transformer model

In an ideal transformer, as shown in Figure 1, all the magnetic flux produced in one winding links all the turns of the second winding. Thus, the voltage and current ratios are [1]:

$$\frac{v_2}{v_1} = \frac{N_S}{N_P} = \frac{1}{n} \quad (1)$$

$$\frac{i_2}{i_1} = -n \quad (2)$$

where N_P and N_S are the number of turns for the primary side and secondary side, respectively. The ideal transformer does not exist in the real world, but is instead affected by a number of parasitic elements.

Lossless transformer model

Actual transformers differ from the ideal transformer in several ways. A schematic of the equivalent model of a lossless transformer model is shown in Figure 2. The low-frequency performance is determined by the permeability of the core material and the number of turns on the windings [2]. The high-frequency performance is limited by the fact that not all of the

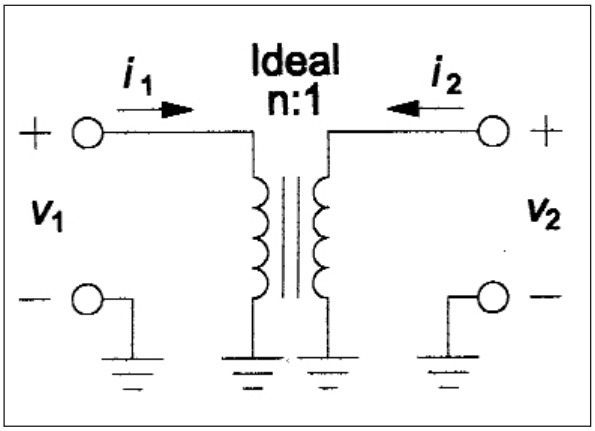

▲ Figure 1. Ideal transformer model.

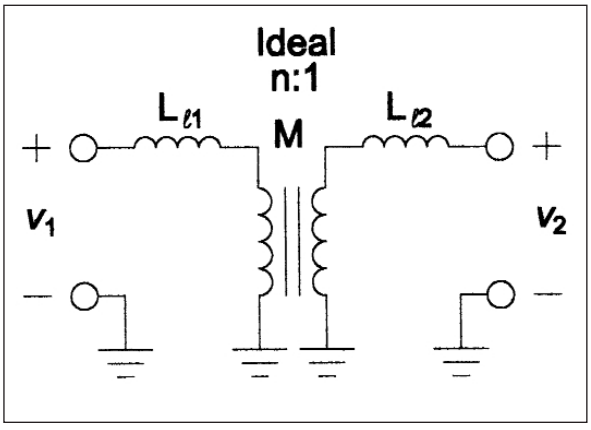

▲ Figure 2. Lossless transformer model.

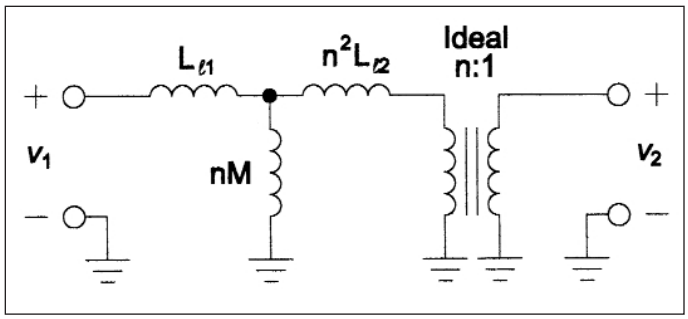

▲ **Figure 3. Lossless transformer model referred to primary side.**

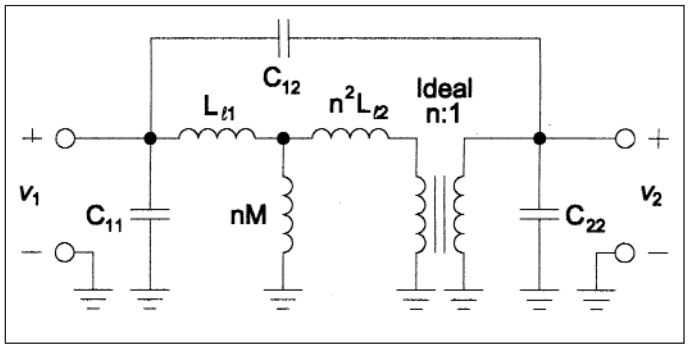

▲ **Figure 4. Wideband transformer model.**

flux produced in one winding links to the second winding, a deficiency known as *leakage* [1].

Since the leakage flux paths are primarily in air, the resultant primary and secondary leakage inductances L_{l1} and L_{l2} are practically constant [3, 4]. A mutual inductance (M) between the two windings is a result of the linked flux in the transformer core. The nonlinearity of the magnetic characteristics of the core material is generally assumed to affect only the relation between the mutual flux and the exciting current. The mutual inductance M is determined by way of:

$$M = \sqrt{L_P L_S k} \tag{3}$$

where L_P and L_S are the primary and secondary winding inductances, which are measured at low frequency with an inductance bridge, leaving the opposite winding open. The coupling coefficient k is then determined by:

$$k = \frac{v_2}{v_1}\sqrt{\frac{L_P}{L_S}} \le 1 \tag{4}$$

where v_1 and v_2 are easily measured across the primary and secondary terminals with a high impedance probe and a network analyzer, an RF sampling voltmeter, or an oscilloscope with the secondary unloaded and at a frequency that is much lower than the first resonant frequency of the transformer [5]. The value of k is always less than one, because perfect coupling between windings is unachievable. The coupling between windings can be improved by such techniques as twisting the wires together, which increases the interwinding capacitance, or the use of coaxial transmission line where the coupling fields are completely contained within the dielectric.

With the mutual inductance known, the leakage inductances L_{l1} and L_{l2} can be determined by way of [4]:

$$L_{l1} = L_P - nM \tag{5}$$

$$L_{l2} = L_S - \frac{M}{n} \tag{6}$$

It is often convenient to describe transformer models from the viewpoint of the primary winding. The model as such for the lossless transformer is described in Figure 3.

Lossless wideband transformer model

The transformer model that has been described so far is adequate for describing low-frequency transformers such as those used at audio frequencies where any parasitic resonances are far outside the frequency range of interest. At higher frequencies, however, these resonances, which are the result of stray capacitances, come into play. The three principle capacitances that define the wideband transformer are shown in Figure 4.

It is generally understood that the capacitances associated with wideband transformers are distributed, but it is inconvenient to model transformers by way of distributed capacitances per se; thus a single lumped capacitance is used.

In Figure 4, capacitor C_{11} represents the distributed primary capacitance, which is a result of the shunt capacitance of the primary winding. Likewise, C_{22} represents the shunt capacitance of the secondary winding. Some models depict these shunt capacitances as a single capacitor in parallel with the mutual inductance nM [6], but such models do not fully describe the resonances experienced in high-frequency transformers. Capacitor C_{12} is referred to as the interwinding capacitance [7], and is also a distributed capacitance. In conjuction with the distributed inductance of the windings, capacitor C_{12} can form a transmission line whose characteristic impedance can be controlled by way of the wire size, insulation thickness, and degree of twisting [8].

As with the earlier model of the lossless transformer, it is convenient to describe the lossless wideband transformer model from the viewpoint of the primary winding, as shown in Figure 5. Here, the three model capacitances are transformed in the following manner [4]:

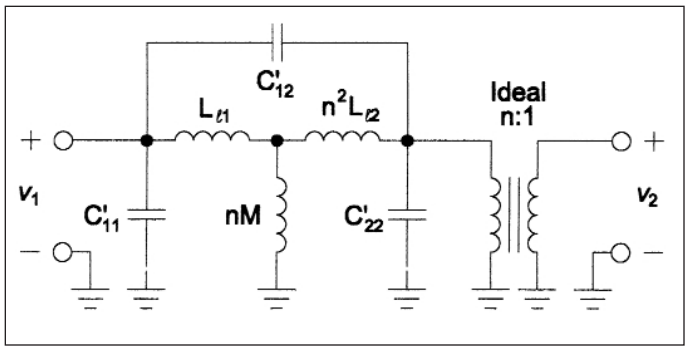

▲ **Figure 5. Wideband transformer model referred to primary side.**

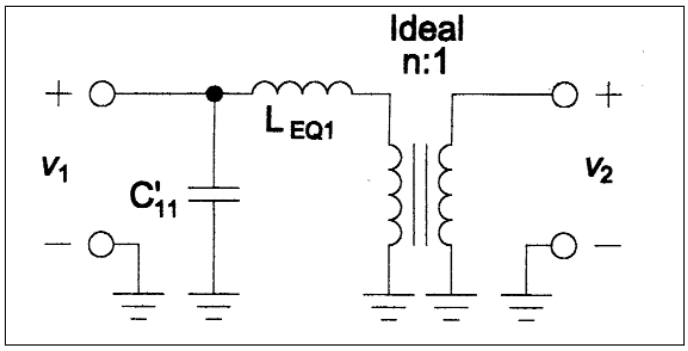

▲ **Figure 6. Equivalent circuit for determining C′12 and C′22.**

$$C'_{11} = C_{11} + C_{12}\left(1 - \frac{1}{n}\right) \tag{7}$$

$$C'_{12} = \frac{C_{12}}{n} \tag{8}$$

$$C'_{22} = \frac{C_{22}}{n^2} + C_{12}\left(\frac{1}{n} - 1\right) \tag{9}$$

In some circumstances, the capacitance C'_{11} may be hypothetically negative [4]. Furthermore, the capacitance C'_{11} is frequently ignored, since its effects are generally unimportant due to its position in the circuit [4]. However, at HF and higher frequencies it should be evaluated to determine its contribution to the high-frequency cutoff point.

Using the equivalent circuit shown in Figure 6, the interwinding capacitance C'_{12} can be determined by first measuring the parallel resonant frequency f_{12} of the unloaded transformer. Begin by connecting an appropriate signal generator to the primary winding of the transformer. Using a high impedance probe with a network analyzer, an RF sampling voltmeter, or an oscilloscope, observe the voltage at the secondary winding while adjusting the frequency of the generator. The resonant frequency f_{12} is the point where the voltage across the secondary winding reaches a null, or minimum.

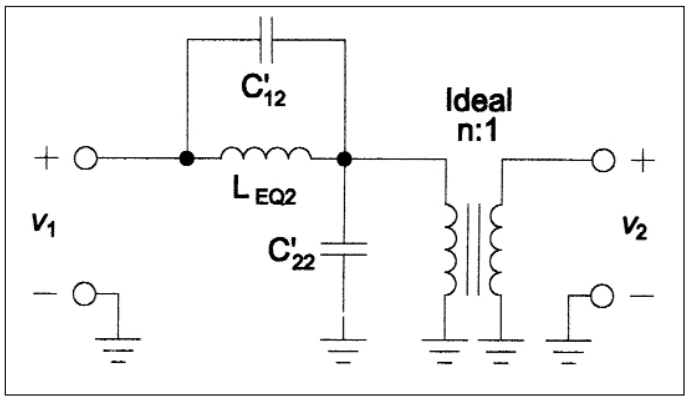

$$C'_{12} = \frac{1}{L_{EQ2}(2\pi f_{12})^2} \tag{10}$$

where the equivalent transformer inductance L_{EQ2} is determined by:

$$L_{EQ2} = \frac{nML_{11}}{nM + L_{11}} + n^2 L_{12} \tag{11}$$

The output shunt capacitance C'_{22} can now be determined by measuring the series resonant frequency f_{22} at the input terminals of the transformer. With the generator still connected to the primary winding, adjust the frequency while observing the voltage across the primary winding. The resonant frequency f_{22} is the point where the voltage across the primary reaches a null, or minimum.

$$C'_{22} = \frac{1 - C'_{12}L_{EQ2}(2\pi f_{22})^2}{L_{EQ2}(2\pi f_{22})^2} \tag{12}$$

In a similar manner, the input shunt capacitance C'_{11} can be determined by measuring the series resonant frequency f_{11} at the output terminals of the transformer. Begin by connecting the signal generator across the seconday winding, leaving the primary winding open. The resonant frequency f_{11} is the point where the voltage across the secondary reaches a null, or minimum.

$$C'_{11} = \frac{1 - C'_{12}L_{EQ1}(2\pi f_{11})^2}{L_{EQ1}(2\pi f_{11})^2} \tag{13}$$

where the equivalent transformer inductance L_{EQ1} is determined by:

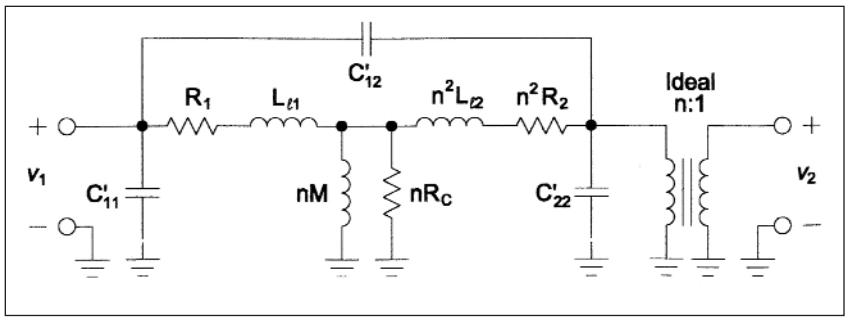

▲ **Figure 8. Complete wideband transformer model.**

$$L_{EQ1} = \frac{n^2 ML_{12}}{M + nL_{12}} + L_{11} \tag{14}$$

Complete equivalent wideband transformer model

No discussion about transformer models is complete without some mention of losses. Two principle loss mechanisms are involved in the wideband transformer: the resistive loss in the copper wires and the hysteresis loss in the ferromagnetic core material. Figure 8 depicts the complete model of the wideband transformer, which has been referred to the primary side earlier. The series resistance R_1 represents the loss associated with the wire in the primary winding. This resistance is nonlinear, increasing with frequency according to $\sqrt{\omega}$ because of the skin effect of the wire itself [5]. Similarly, the series resistance R_2 represents the loss associated with the wire in the secondary winding. Due to the short wire length used in wideband transformers having ferromagnetic cores, the contribution of the resistive loss to the total loss is small and is therefore generally omitted [5].

The shunt resistance R_C represents the hysteresis loss due to the ferromagnetic core [9], which increases with ω^2 or even ω^3, and is significant in transformers that are operated near the ferroresonance of the core material [5]. In general, this is not a problem provided that proper consideration is given to the selection of the core material.

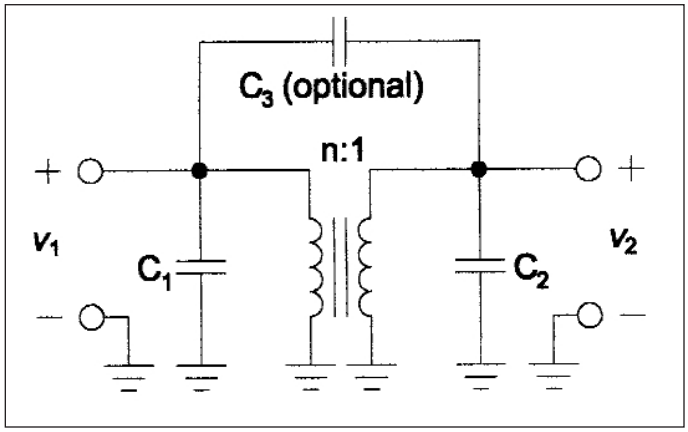

▲ **Figure 9. Matching network components.**

Generally, the factors which affect the insertion losses of the wideband transformer at lower frequencies, attributed to the permeability of the core material and the amount of wire in the windings [2], have a negligible effect in the higher frequency regions [9]. At the same time, the factors associated with losses at higher frequencies, attributed to the skin effect of the wire and the ferroresonance of the core material, have a negligible effect at the lower frequencies [9]. At midband frequencies, losses are more likely to be a result of impedance mismatches.

Wideband transformer as a matching network component

Using a wideband transformer at HF and especially VHF frequencies without compensation is poor design practice. The series inductance alone is sufficient to reduce the high-end performance, and the capacitances do not make things much better. Therefore, we consider the equivalent series inductance of the transformer as being the series inductor of a 3-pole lowpass filter. We then add appropriate capacitors to the input and output and possibly one from the input to the output to complete a wideband matching network with minimal loss.

For the purpose of including the transformer inductance as an element in a wideband matching network, we first recognize that this equivalent inductance determines the maximum usable frequency ω_{max} for the matching network. Therefore, we begin by determining ω_{max} by:

$$\omega_{max} = \frac{L_{norm} R_S}{L_{EQ1}} \tag{15}$$

where R_S is the source impedance of the generator and L_{norm} is the normalized inductance of the lowpass filter section that will be used. A fairly complete listing of the protoype values for a wide range of filter approximations is shown in Table 1 [10, 11]. The added input and output capacitances C_1 and C_2 are determined by:

$$C_1 = \frac{C_{1norm}}{\omega_{max} R_S} - C_{11} \tag{16}$$

$$C_2 = \frac{n^2 C_{2norm}}{\omega_{max} R_S} - C_{22} \tag{17}$$

where C_{1norm} and C_{2norm} are the normalized input and output capacitances of the lowpass filter section, also listed in Table 1. Except for Bessel and Gaussian filter

sections, which are time delay filters [12], the prototype values for C_{1norm} and C_{2norm} are identical.

In some cases, it may be desireable to make an Inverse Tchebychev or elliptical filter section, such as in the case where additional close-in harmonic energy needs additional suppression, keeping in mind that the group delay variations in the vicinity of the cutoff frequency are more severe than for other filter types. In such a situation, an additional capacitance can be included from the input to the output of the transformer:

$$C_3 = \frac{nC_{3norm}}{\omega_{max} R_S} - C_{12} \quad (18)$$

Note that the transformer must be symmetrical, i.e., either noninverting unbalanced to un-balanced or balanced to balanced.

Design procedure summary

- Using an inductance bridge, measure the primary and secondary winding inductances L_P and L_S.
- Using a signal generator, and a high impedance probe with a network analyzer, a sampling RF voltmeter, or an oscilloscope, measure the input and output voltages v_1 and v_2 at an approriate midband frequency.
- Calculate the coupling coefficient k using Equation (4) and the mutual inductance M using Equation (3).
- Calculate the primary and secondary leakage inductances L_{l1} and L_{l2} using Equations (5) and (6), respectively.
- Calculate the equivalent inductances L_{EQ1} and L_{EQ2} using Equations (14) and (11), respectively.
- Continuing with the test setup described in (2), measure the transmission parallel resonant frequency f_{12}, the input series resonant frequency f_{11}, and the output series resonant frequency f_{22}.
- Calculate C'_{12}, C'_{22} and C'_{11} using Equations (10), (12) and (13), respectively.
- Calculate C_{12}, C_{11} and C_{22} using Equations (8), (7) and (9), respectively.
- Select a filter prototype from Table 1.
- Calculate the maximum usable frequency ω_{max} using Equation (15).
- Calculate the values for the input and output matching capacitors C_1 and C_2 using Equation (16) and (17), respectively.
- If required, calculate the value for the capacitor C_3 using Equation (18).

Filter Type	C_{1norm}	C_{2norm}	L_{norm}	C_{3norm}
Butterworth	1.000	1.000	2.000	
Bessel	1.255	0.192	0.553	
Gaussian	2.196	0.967	0.336	
Tchebyschev				
0.1dB	1.032	1.032	1.147	
0.5dB	1.596	1.596	1.097	
1.0dB	2.024	2.024	0.994	
Inverse Tchebyschev				
20dB	1.172	1.172	2.343	0.320
30dB	1.866	1.866	3.733	0.201
40dB	2.838	2.838	5.677	0.132
Elliptical (0.1dB Passband Ripple)				
20dB	0.850	0.850	0.871	0.290
25dB	0.902	0.902	0.951	0.188
30dB	0.941	0.941	1.012	0.125
35dB	0.958	0.958	1.057	0.837
40dB	0.988	0.988	1.081	0.057
Elliptical (0.5dB Passband Ripple)				
20dB	1.267	1.267	0.748	0.536
25dB	1.361	1.361	0.853	0.344
30dB	1.425	1.425	0.924	0.226
35dB	1.479	1.479	0.976	0.152
40dB	1.514	1.514	1.015	0.102
Elliptical (1.0dB Passband Ripple)				
20dB	1.570	1.570	0.613	0.805
25dB	1.688	1.688	0.729	0.497
30dB	1.783	1.783	0.812	0.322
35dB	1.852	1.852	0.865	0.214
40dB	1.910	1.910	0.905	0.154

▲ **Table 1. Matching section prototype values.**

Conclusion

Many considerations influence the design of circuits employing wideband transformers. It is not sufficient to conclude the design by simply choosing the wire and the core material to be used. The parasitic inductive and capacitive reactances that accompany the transformer must be considered in the overall circuit design in order to realize the best possible performance. The transformer models and equivalent circuits presented here should help the designer gain an intuitive understanding of the nature of these reactances and their impact on the circuits in which they are to be used. The procedure shown should give the designer a brief but thorough methodology for analyzing the transformers at hand and then completing the circuit design with the transformer parasitics incorporated in a broadband matching circuit with minimal losses. ■

References

1. Bruce D. Wedlock and James K. Roberge, *Electronic Components and Measurements*, Englewood Cliffs N.J.: Prentice-Hall, 1969.

2. G. R. Haack, "Common-Mode Resonance Effects in High Frequency RF Transformers (Baluns)," *Proceedings of the 19th International Electronics Convention and Exhibition (IREECON 83)*, 1983.

3. Leander W. Matsch, *Capacitors, Magnetic Circuits and Transformers*, Englewood Cliffs, N.J.: Prentice-Hall, 1964.

4. MIT Department of Electrical Engineering, *Magnetic Circuits and Transformers*, New York: John Wiley, 1943.

5. P. Kreuzgruber, et al, "Modeling of Three-Port RF Transformers," *IEE Proceedings*, Part G, Vol. 138, No. 3, June 1991.

6. William M. Flanagan, *Handbook of Transformer Design and Applications*, Second Edition, New York: McGraw-Hill, 1992.

7. Thomas R. O'Meara, "Analysis and Synthesis with the 'Complete' Equivalent Circuit for the Wide-Band Transformer," *Transactions of the AIEE*, Part I, March 1962.

8. Peter Lefferson, "Twisted Magnet Wire Transmission Line," *IEEE Transactions on Parts, Hybrids and Packaging*, Vol. 7, No. 4, December 1971.

9. E. C. Snelling, *Soft Ferrites: Properties and Applications*, Second Edition, Butterworths, 1988.

10. A. H. Hilbers, "Design of High-Frequency Wideband Power Transformers," *Electronic Applications*, Vol. 32, No. 1, January 1973, later reprinted as Philips Application Note ECO7213.

11. Philip R. Geffe, *Simplified Modern Filter Design*, New York: Rider, 1963.

12. Lawrence P. Huelsman, *Active and Passive Analog Filter Design: An Introduction*, New York: McGraw-Hill, 1993.

13. Herman J. Blinchikoff and Anatol I. Zverev, *Filtering in the Time and Frequency Domains*, Norcross, GA: Noble Publishing Corporation, 1987.

Author information

Chris Trask is a principal engineer at Sonoran Radio Research in Tempe, AZ. He also works as an RF and microwave consultant. He received bachelor of science and master of science degrees in electrical engineering from The Pennsylvania State University. He has published 13 papers and holds nine patents. He can be reached via E-mail: ctrask@qwest.net; or Tel: 480-966-7395.